Astro2020 Science White Paper

Surveying the solar neighborhood for ozone in the UV at temperate rocky exoplanets

Thematic Area: Planetary Systems

Principal Author:
Name: Doug Lisman
Institution: Jet Propulsion Laboratory, California Institute of Technology
Email: d.lisman@jpl.nasa.gov
Phone: 626-773-6133

Co-authors:
Edward W. Schwieterman, University of California, Riverside

Christopher T. Reinhard, Georgia Institute of Technology
Stephanie L. Olson, University of Chicago
Timothy W. Lyons, Stephen Kane: University of California Riverside
Patrick Cote', NRC-Herzberg
Tony Hull, University of New Mexico
Sara R. Heap, Emerita Scientist, Goddard Space Flight Center
John C. Mather, Eliad Peretz: Goddard Space Flight Center
Bertrand Mennesson, Jason Rhodes, Stuart B. Shaklan: Jet Propulsion Laboratory

Abstract:

In this whitepaper we show that the potential biosignature gas ozone enables a compelling early exoplanet imaging mission that can be launch ready in the next decade. While oxygen remained at undetectably low levels over much of Earth's evolutionary history, its proxy ozone has a pronounced absorption feature in the UV for about half of that history. Compared to the oxygen A-Band at present atmospheric levels, ozone's Hartley-Huggins band generally contains more in-band stellar flux and can be detected at much lower SNR. We present a proof of concept mission that pairs a 20-m starshade, matching current prototype sizes, with a 1-1.5 m UV telescope, potentially provided by an international partner, and a photometer instrument. The combination of a starshade and telescope observing in the UV leads to a smaller inner working angle and improves planet sensitivity through a reduced point spread function solid angle. This mission is expected to detect at least one temperate rocky planet with high confidence. It will also significantly inform planetary system diversity and exozodiacal light levels. An early small mission would smooth the way for a successful flagship mission, with much reduced risk, and potentially identify compelling targets for the flagship mission to follow-up on.

1. Introduction

This paper first outlines the evolutionary history of oxygen on Earth and makes the case for ozone as a potential biosignature gas that is thought to be at detectable levels for much of that history. It then goes on to show that a focus on detecting ozone in the UV at temperate rocky planets enables a compelling low-cost space mission that can be launch ready in the next decade. This paper outlines science objectives, defines a proof of concept mission and then evaluates its performance. Finally, clear conclusions are reached and a path forward is recommended.

A flagship space mission is required to detect exoplanet biosignatures with high confidence (Gaudi et al. 2018). To smooth the way for a successful flagship mission with manageable risk, we propose an early small mission that works out myriad flight design details at a smaller scale first and, critically, at a smaller burn-rate of funds. This early mission adopts the more modest goal to detect a "potential biosignature gas", which means that a biologic origin is likely, but not necessarily certain. This mission will also provide unprecedented broadband exoplanet imaging, to advance our understanding of exozodiacal dust levels (exozodi) and planetary system diversity.

A starshade is adopted here as the only viable starlight suppression technology for observing in the UV at present. Starshade and telescope performance both improve at shorter wavelengths.

2. The history of oxygen on Earth and the case for ozone

The most drastic chemical impact of life on Earth is the significant amount of molecular oxygen (O_2) in the atmosphere, constituting 21% by volume in the modern era. Oxygen has long been considered a potential exoplanet biosignature given its almost exclusive production by photosynthetic life on our planet, strong chemical reactivity, and identifiable spectral signatures in the optical-NIR (see review in Meadows et al. [2018]). Indeed, a photosynthetic biosphere that produces oxygen is also more likely to be detectable because the most basic ingredients of this metabolism (H_2O, CO_2, and photons) are likely abundant in planetary environments and allows higher productivity than possible chemosynthetic or anoxygenic biospheres (Des Marais 2000). The major spectral features of O_2 are located at wavelengths of 630 nm (O_2-γ), 690 nm (O_2-B), 760 nm (O_2-A), and 1.27 μm. For similar reasons, oxygen's photochemical byproduct ozone (O_3) is also suggested as an exoplanet biosignature (Leger et al. 1993; Segura et al. 2003), producing strong absorption features at UV (200-300 nm), visible (the broad 500-700 nm Chappuis band), and mid-infrared (9.65 μm) wavelengths. Of these, the Hartley-Huggins band in the UV centered at 250 nm is by far the most sensitive to low O_2 levels, saturating at O_3 abundances of ~1 ppmv, corresponding to O_2 fractions of ~1% of present atmospheric level (PAL) (Reinhard et al. 2017; Schwieterman et al. 2018.

The history of the oxygenation of Earth's atmosphere is multifaceted and remains under intense study (Lyons et al. 2014; Olson et al. 2018b). However, data from Earth's geochemical archive provide convincing evidence for three distinct phases with atmospheric O_2 levels near modern levels for only the last 10% of our planet's history, as shown in Figure 1. Prior to the Great Oxidation Event (GOE) at 2.33 Ga (Luo et al. 2016), geochemical proxy data derived from sulfur mass-independent-fraction suggests $pO_2 < 10^{-5}$ PAL (Zahnle et al. 2006) and photochemical

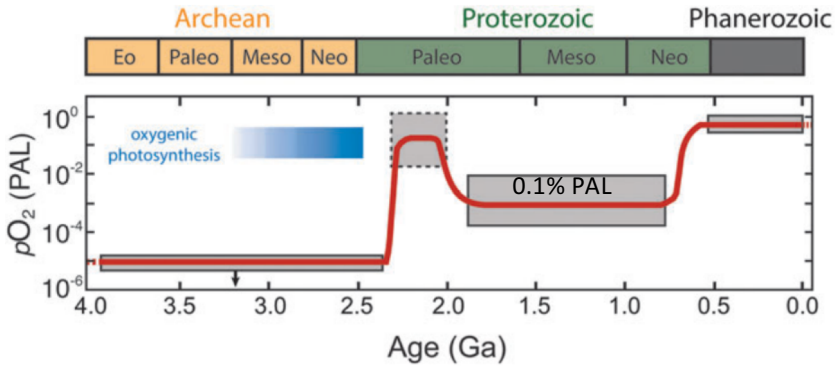

Figure 1: A schematic history of oxygen on Earth from Schwieterman et al. 2018b

models suggest even lower O_2 values, perhaps by orders of magnitude (Claire et al. 2006; Goldblatt et al. 2009). During the Proterozoic Eon (2.5-0.54 Ga), a possible "O_2 overshoot" from the GOE gave way to pO_2 levels substantially higher than in the Archean, but far below modern. The precise abundance of pO_2 during this time is disputed, and likely varied with time. Evidence from the isotopic fractionation of Chromium isotopes suggest pO_2 > 0.1% PAL (Planavsky et al. 2018, 2014), while other estimates range up to 10-40% (Kump 2008). During the last 541 million years pO_2 levels have stabilized near modern values within a factor of ~2, concurrent with the great expansion and diversification of animal life on Earth (Reinhard et al. 2016).

If the chemical evolution of Earth's atmosphere provides a guide for exoplanets, then we may expect many to possess O_2 levels below the detection limits for the O_2-A band (Reinhard et al. 2017). ***However, for even the lowest oxygen concentrations predicted for the Proterozoic Earth, the Hartley-Huggins ozone band would have generated a significant spectral signature*** (Olson et al. 2018a), making UV observations of ozone a sensitive probe to atmospheric oxygenation even at low pO_2. Figure 2a illustrates the impact on the UV O_3 band as pO_2 is lowered. At concentrations > 1% PAL, decreased pO_2 results in shorter UV cutoff wavelengths until the predicted O_3 abundances drop sufficiently that the band is no longer saturated at 250 nm. Our results here show that significant absorption is still present even for O_2 concentrations of tens of ppm. For this reason, single-band detection of ozone is less susceptible to false negatives than the O_2-A band, which shows negligible absorption at these low O_2 values, as shown in Figure 2b.

Many recent papers have examined the possibility of abiotic O_2 accumulation in terrestrial planet atmospheres, generating potential false positives for a photosynthetic biosphere (see reviews in Meadows 2017; Harman and Domagal-Goldman 2018). Most false positive scenarios for detectable O_2 are relevant for habitable zone (HZ) planets orbiting M dwarfs (e.g., Luger and Barnes 2015), which do not possess sufficient angular separations from their host stars to be relevant for this proposed survey. However, some early results suggest photolysis of CO_2 and H_2O, in terrestrial exoplanet atmospheres with low H contents, may produce detectable O_3 for planets orbiting F or K dwarf stars (Domagal-Goldman et al. 2014; Harman et al. 2015). A recent study suggests that the presence of lightning, producing NO_x molecules, would effectively catalyze combination of CO and O_2 into CO_2, negating this particular false positive possibility (Harman et al. 2018). Rarefied atmospheres lacking a tropospheric cold trap for H_2O

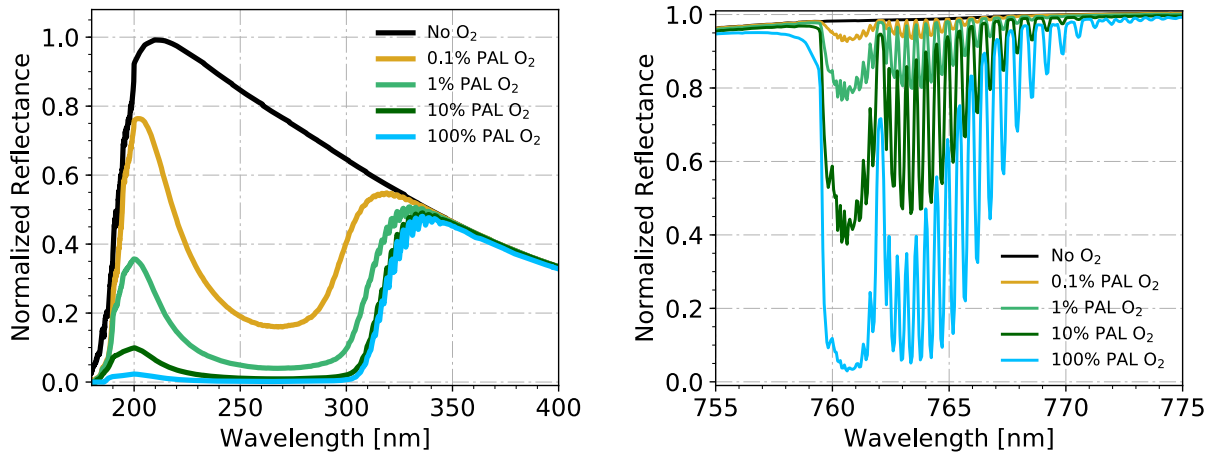

Figure 2: (a) synthetic spectra illustrating pO_2-dependent absorption by the O_3 Hartley-Huggins bands, (b) absorption by the O_2-A band as a function of pO_2. The UV O_3 band is much more sensitive to low pO_2 than the O_2-A band.

may also produce abiotic O_2/O_3 through the efficient photolysis of H_2O in the stratosphere (Wordsworth & Pierrehumbert 2014). We do not dwell overly on false positive scenarios here because we acknowledge that *single band ozone detection (or any molecule, including O_2) is insufficient information to claim a certain detection of life.* However, identifying an ozone signature on a habitable zone exoplanet in the solar neighborhood would provide an extremely compelling case for follow-up observations. Multiple detections of ozone in the target population may provide statistical evidence for the presence of life depending on context (Bean et al. 2017).

In summary, the known chemical and spectral properties of atmospheric ozone, combined with our knowledge of the compositional evolution of Earth's atmosphere over geologic time, suggest the intrinsic yield of detectable ozone signatures is higher than for other potential biosignature gases, like oxygen. These factors, along with the technical advantages to searching at UV wavelengths discussed below, compel us to select ozone as the target biosignature gas for a small, low-cost starshade mission.

3. Proposed science objectives

The primary and driving science objective is to detect with high confidence at least one temperate rocky planet and to identify the presence of ozone in detected rocky planet atmospheres. Other exciting objectives, more directly achieved with broadband imaging, are to characterize exozodi levels and planetary system diversity. An unprecedented imaging capability will significantly expand our database of exoplanets to include smaller planets and planets in longer period orbits. The estimated composite occurrence rate for likely rocky planet sizes between 1.16 and 1.77 R_E is about 20% (Fulton et al. 2017). From this, we derive the goal to search at least 5 cumulative HZs.

4. Proof of concept mission

The concept of an early small starshade mission focused on detecting ozone in the UV was first studied for the Occulting Ozone Observatory (O_3) (Savransky et al. 2010). Searching for the broad and deep O_3 feature from 200-310 nm enables this small mission approach in several ways. It can

be identified via photometer at a low SNR of 5, with respect to the continuum. While stellar spectra weaken to the blue side of the blackbody peak, the integrated in-band flux is greater for the ozone band than for the O_2 A-Band (752-768 nm), for every star but the two coolest target stars. The combination of a starshade and telescope observing in the UV leads to a tighter inner working angle (IWA) and improves planet sensitivity through a reduced point spread function solid angle.

Our goal is to leverage a small UV telescope with separate science objectives and, preferably, separate funding. A dedicated photometer instrument detects ozone at 200-310 nm and the continuum at 310-450 nm. A δ-doped analog mode CCD detector gives detective quantum efficiency (dQE) of ~35% (Scott et al. 2014). Detector read-noise at ~3 electrons per pixel is mitigated by binning on-chip the critical ozone channel down to 1 pixel per λ/D spot. A photon counting detector at lower dQE is only advantageous at low exozodi density (<~2X local zodi).

The starshade in all cases is 20-m in total diameter. A 6-m petal length matches current TRL5 prototypes. An 8-m disk diameter is smaller than current 10-m TRL5 prototypes. Carrying current sizes all the way to flight significantly reduces cost and risk. The starshade and telescope co-launch on a Falcon-9 launch vehicle to Earth-Sun L2. The starshade spacecraft performs propulsive maneuvers to line up on target stars with conventional biprop technology. We expect to search ~16 stars in broadband mode in year 1 and then return to select targets to search for ozone and constrain exoplanet orbits. The target mission cost is below the $610M Exo-S team estimate (Seager et al. 2015), based on a 30-m starshade, Class B mission and analogies to the WISE Explorer Mission.

Two UV telescope designs are considered. First, is a 1-m off-axis design, operating at 82.5 mas IWA, with 47% optical throughput within λ/D. A candidate telescope is the Canadian Space Agency's (CSA) CASTOR Mission, that is potentially free to NASA via an international mission partnering agreement. Second, is a 1.5-m on-axis design, operating at 69 mas IWA, with 25% optical throughput within λ/D. A candidate telescope is the CETUS Probe Study Mission.

5. **Performance evaluation**

We now evaluate the performance of these two telescope options against the goal to search ≥ 5 HZs. We apply this goal in the presence of the estimated median exozodi density of 4.5 times local zodi (Mennesson, 2019) at all stars. We reduce the total yield by 20% to account for ~30% of stars that have much higher exozodi. We conservatively consider only single observations in characterization mode, but recognize that a modest improvement is possible with additional observations. We assume that stars with a predicted search completeness < 20% are not observed. We apply a local zodi brightness of 22 mags/arc-sec^2 that relates to a 60° average orbit inclination.

Critical performance parameters of IWA and planet contrast sensitivity constrain the detectable region within the HZ, defined as $0.95AU\sqrt{L}$ to $1.67AU\sqrt{L}$, where L is stellar bolometric luminosity relative to Sun (Kopparapu et al. 2013). Planet contrast (C_p) is the ratio of planet flux to the known unsuppressed star flux and follows the equation: $C_p \geq ipR^2/a^2$. The illumination factor (i) follows a Lambertian phase function. The geometric albedo (p) of 0.2 matches Earth. We randomly assign to each star the midpoint of the 4 smallest radius (R) bins (1.23, 1.36, 1.51, 1.68 R_E) consistent with the estimated size population distribution (Fulton et al. 2017). Planet contrast for a given star and exozodi level is constrained by 3 primary factors: 1) planets can be no dimmer than 30 visual

magnitudes, per the noise floor; 2) integration time per star is ≤ 25 days, per Sun constraints and 3) planet flux is ≥ 10% of exozodi flux, per the expected exozodi calibration accuracy.

Critical star parameters of Earth distance (d) and bolometric luminosity relative to Sun (L) limit planet contrast sensitivity, per the factor d^2/L, as shown in Figure 3 for 18 nearby and mostly Sun-like (F, G, K) stars. We compute HZ search completeness as a numerical integral of detection probability in concentric shells. A shell weighting factor accounts for the logarithmic planet distribution with semi-major axis(a). Figure 4 shows the total *characterized* HZs as a function of exozodi density and telescope design.

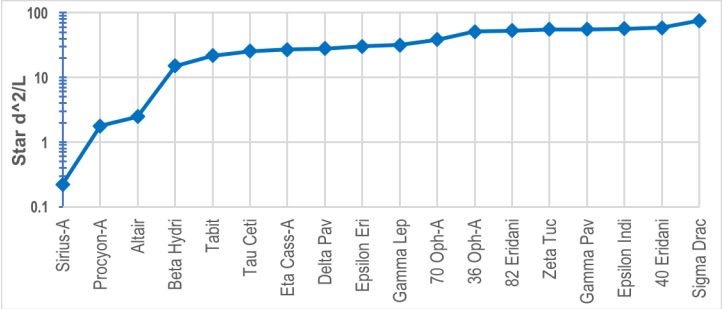

Figure 3: Planet contrast sensitivity has a large dynamic range due to the star factor d^2/L, which limits the target list. Note that we only observe binary stars with sufficiently dim and separated partners.

6. Conclusions

Ozone is a robust potential biosignature gas that is detectable at temperate rocky planets with a small, relatively low-cost mission (20-m starshade, 1-1.5 m UV telescope, photometer instrument) that can be launch-ready in the next decade. This mission has high confidence to detect at least one temperate rocky planet and identify atmospheric ozone that corresponds to oxygen concentration as low as ~0.1% of PAL, as thought to be present at Earth since 2.3 Ga. Broadband imaging will also detect a diverse array of planet size and orbital period and inform exozodi levels. This mission will smooth the way for a successful flagship mission by mitigating significant risk and possibly identifying targets for further observation. Candidate 1-1.5 m UV telescopes, under study for separate science missions, can be leveraged. One candidate telescope is potentially provided by an international partner.

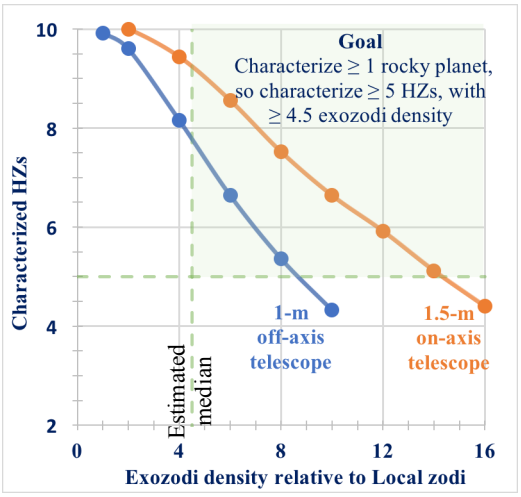

Figure 4: Characterized HZs vs. exozodi density & telescope design. Yields converge at low density as yield becomes target limited and detector read-noise starts to dominate integration times. Broadband detection yield (not shown) is higher at densities < 4-5, but converges with characterized yield at higher density as the exozodi calibration accuracy starts to dominate integration times.

7. Recommendations

We recommend an early small starshade mission in the next decade to image exoplanets and search for ozone in the UV in the atmospheres of temperate rocky planets with a 1-1.5 m UV telescope. We recommend further study of mission implementation, including cost, launch readiness date, mission performance simulations and telescope accommodations. We also recommend further study and modeling of the geologic and geochemical evolution of Earth's historical atmosphere and possible planet variations.

References

Bean, J. L., Abbot, D. S., & Kempton, E. M.-R. 2017, *ApJ*, 841, L24
Claire, M. W., Catling, D. C., & Zahnle, K. J. 2006, *Geobiology*, 4, 239–269
Domagal-Goldman, S. D., Segura, A., Claire, M. W., et al. 2014, *ApJ*, 792, 43
Fulton, B. J., Petigura, E. A., Howard, A. W., et al. 2017, AJ, 154:109
Gaudi, B. S., Seager, S., et al. 2018, The Habitable Exoplanet Observatory Mission Concept Study Interim Report
Goldblatt, C., Watson, A. J., & Lento, T. M. 2009, *Bioastronomy 2007: Molecules*, 420,
Harman, C. E., Schwieterman, E. W., Schottelkotte, J. C., et al. 2015, *ApJ*, 812, 137
Harman, C. E., Felton, R., Hu, R., et al. 2018, *ApJ*, 866, 56
Harman, C. E. & Domagal-Goldman, S. in Springer International Publishing, 2018, *Handbook of Exoplanets*, 1–22
Kopparapu, R. K., et al. 2013, ApJ 765(2): p. 131
Kump, L. R. 2008, *Natur*, 451, 277–278
Leger, A., Pirre, M., & Marceau, F. J. 1993, *A&A*, 277, 309
Luger, R. & Barnes, R. 2015, *AsBio*, 15, 119–143
Luo, G., Ono, S., Beukes, N. J., et al. 2016, *Science Advances*, 2, e1600134–e1600134
Lyons, T. W., Reinhard, C. T., & Planavsky, N. J. 2014, *Natur*, 506, 307–15
Marais, D. 2000, *Sci*, 289, 1703–1705
Meadows, V. S. 2017, *AsBio*, 17, 1022–1052
Meadows, V. S., Reinhard, C. T., Arney, G. N., et al. 2018, *AsBio*, 18, 630–662
Mennesson, B. 2019, personal communication
Olson, S. L., Schwieterman, E. W., Reinhard, C. T., et al. 2018a, *ApJL*, 858, L14
Olson, S. L., Schwieterman, E. W., Reinhard, C. T., et al. in (Deeg, H. & Belmont, J.) Springer International Publishing, 2018b, *Handbook of Exoplanets*, 1–37
Planavsky, N. J., Cole, D. B., Isson, T. T., et al. 2018, *Emerging Topics in Life Sciences*, ETLS20170161
Planavsky, N. J., Reinhard, C. T., Wang, X., et al. 2014, *Sci*, 346, 635–638
Reinhard, C. T., Olson, S. L., Schwieterman, E. W., et al. 2017, *AsBio*, 17, 287–297
Reinhard, C. T., Planavsky, N. J., Olson, S. L., et al. 2016, *PNAS*, 113, 8933–8938
Savransky, D., Spergel, D. N., Kasdin, N. J., Cady, E. J. et al. 2010, SPIE Vol. 7731: 2H-1
Schwieterman, E., Reinhard, C., Olson, S., et al. 2018, *arXiv preprint 1801.02744*,
Scott, A. D., Cote', P., Rowlands, N., Daigle, O., 2014, SPIE Vol. 91542C-2
Seager, S. et al. 2015, Exo-S Starshade Probe-Class STDT Report
Segura, A., Krelove, K., Kasting, J. F., et al. 2003, *AsBio*, 3, 689–708
Wordsworth, R. & Pierrehumbert, R. 2014, *ApJ*, 785, L20
Zahnle, K., Claire, M., & Catling, D. 2006, *Geobiology*, 4, 271–283